

# Passivation Characteristics of New Silicon Oxide

Lei Gong, Chunlan Zhou, Junjie Zhu, Wenjing Wang

**Abstract**—Surface passivation on silicon is one of the hot topics for research in the field of silicon solar cells. Single layers of silicon oxide prepared by thermal oxidation, O<sub>3</sub> oxidation or chemical oxidation and the stack layer of silicon oxide combined with other dielectric layers as passivation layers have been widely used to reduce surface carrier recombination in silicon solar cells. This paper provides a new method for preparing silicon oxide that realizes an excellent passivation effect, in which perhydropolysilazane was used as a spin-coating precursor. The effective minority carrier lifetime for n-type silicon passivated by a SiO<sub>x</sub> layer increases with SiO<sub>x</sub> thickness and can reach 1 ms when thickness is up to 100 nm. Moreover, when SiO<sub>x</sub> layers with a thickness of 100 nm or more were capped by an AlO<sub>x</sub> or SiN<sub>x</sub> layer, the effective minority carrier lifetime could get a value above 2 ms, which is much higher than the value for single SiN<sub>x</sub> or AlO<sub>x</sub> (approximately 500–750 μs). This may result from the high positive fixed charge in the SiO<sub>x</sub> layer and high hydrogenation of silicon surface induced by H diffusion from AlO<sub>x</sub> or SiN<sub>x</sub> to SiO<sub>x</sub> and stored in it.

**Index Terms**—interface fixed charge, passivation, perhydropolysilazane, silicon oxide

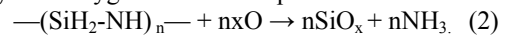
## I. INTRODUCTION

At the silicon solar cell surface, due to the destruction of the crystal periodic structure, dangling bonds are generated, forming defect levels in the forbidden band, which seriously affect the minority carrier lifetime[1]. With the thickness of silicon solar cells continuing to decrease in order to save cost, the diffusion length of minority carriers may be close to or even larger than the thickness of the wafer; so, some carriers will diffuse to the surface to recombine, leading to surface passivation on silicon more important than before. Surface recombination is realized by a combination of the electric field effect and chemical components[2]. The fixed charge  $Q_f$  in the passivation film forms an electric field on the surface of the substrate, causing the energy band to bend and inhibit the movement of the minority carrier to the surface, thus leading to the field-effect passivation; however, the dangling bonds can be saturated by hydrogen atoms during the preparation and annealing of the passivation layers, reducing the interface state density  $D_{it}$  and increasing the minority carrier lifetime. SiN<sub>x</sub>, AlO<sub>x</sub> and SiO<sub>x</sub> are widely used as passivation materials [3-5]. Additionally, Si-SiO<sub>2</sub> has a lattice-matched interface and

positive  $Q_f$  to provide chemical passivation and field-effect passivation, respectively [6, 7]. Most of the silicon solar cells adopt a multi-layer film structure to ensure both the passivation and anti-reflection in practical applications.

The most popular preparation methods of silicon oxide include thermal oxidation, wet chemical oxidation, plasma-enhanced chemical vapor deposition (PECVD), and plasma oxidation [8-10]. Thermal oxidation requires high temperature at 900–1200 °C; silicon atoms on the silicon surface are oxidized to SiO<sub>2</sub> in different atmospheres. However, the thermal oxidation requires large energy consumption, and the oxidation of the silicon wafer generates self-gap silicon atoms and form bulk defects. Wet chemical oxidation mainly includes H<sub>2</sub>O<sub>2</sub>, H<sub>2</sub>SO<sub>4</sub>, and HNO<sub>3</sub> oxidants[11]. The low growth rate of the wet chemical oxidation layer limits its application range, and using oxidants such as HNO<sub>3</sub> requires treatment of the waste, which increases the cost and could be harmful to the ecological environment. PECVD uses SiH<sub>4</sub> and N<sub>2</sub>O or O<sub>2</sub> as a precursor to grow silicon oxide on the substrate, which requires a vacuum environment and a complicated process. In this paper, we use perhydropolysilazane (PHPS) as the spin-coating precursor to prepare a silicon oxide film, it is a low-temperature and uncomplicated process.

PHPS is mainly composed of Si–N and Si–H. It is mainly used for ceramic precursors, ceramic matrix composites and coating materials[12]. PHPS can be cured in an ultraviolet environment, and the  $-(SiH_2-NH)-$  unit undergoes a hydrolysis reaction to form ammonia gas and Si(OH)<sub>4</sub> as an intermediate state[13]. During the subsequent heat treatment, portions of O and H overflow such that Si(OH)<sub>4</sub> forms a SiO<sub>x</sub> grid. The principle of hydrolysis reaction is as follows[12]:  
 $-(SiH_2-NH)-_n + 4nH_2O \rightarrow nSi(OH)_4 + 2nH_2 + nNH_3$ . (1)  
 It can also be cured at appropriate temperature and form SiO<sub>x</sub> directly with oxygen in the atmosphere:



Nagayoshi introduced a 100 nm SiO<sub>x</sub> film which was made from the PHPS precursor into TiO<sub>2</sub> back reflector to promote the surface passivation on silicon[14], but that film is seldom used in solar cells. In this work, we explore the spin coating of a SiO<sub>x</sub> film from a precursor of PHPS for surface passivation. We have studied the effect of annealing temperature and thickness of SiO<sub>x</sub> films on the chemical component. In addition, the contribution of a single SiO<sub>x</sub> layer on silicon surface passivation has been discussed. Finally, double layers of SiO<sub>x</sub>/AlO<sub>x</sub>:H, or SiN<sub>x</sub>/SiO<sub>x</sub>:H made by capping the SiO<sub>x</sub> layer with plasma-enhanced atomic layer deposition (PE-ALD) AlO<sub>x</sub> and PECVD SiN<sub>x</sub> layers were investigated. The result shows that improvements were observed in the two stacks compared to the single passivation layer of SiO<sub>x</sub>, AlO<sub>x</sub>, and SiN<sub>x</sub>.

This work was supported by the research project 61874120 supported by National Natural Science Foundation of China and the research project 261574 granted by Norwegian Research Council.

L. Gong, C.L. Zhou and W.J. Wang are with the Key Laboratory of Solar Thermal Energy and Photovoltaic System, Institute of Electrical Engineering, Chinese Academy of Science (CAS), Beijing 100190, PR China and University of Chinese Academy of Sciences, Beijing 100190, PR China (e-mail: gonglei@mail.iee.ac.cn; zhouchl@mail.iee.ac.cn; wangwj@mail.iee.ac.cn).

J.J. Zhu is with the Solar Energy Department, Institute for Energy Technology, Kjeller, Norway (e-mail: Junjie.Zhu@ife.no).

## II. EXPERIMENTS

In this experiment, a silicon oxide film was formed by spin-coating a PHPS film on Si (100) substrates and using annealing at moderate temperature in atmosphere. An N-type double-sided polished c-Si substrate was adopted with resistivity of 1~10  $\Omega \cdot \text{cm}$ . First, a wafer was immersed in  $\text{H}_2\text{SO}_4:\text{H}_2\text{O}_2 = 4:1$  (volume ratio) at 85  $^\circ\text{C}$  for 10 min and rinsed in DI water; finally, the surface oxide layer was removed using 1% HF. After being dried in  $\text{N}_2$ , PHPS which was diluted with n-butyl ether, was double-sided coated on the silicon surface at 4500 r/min for 60 s by the spin-coating process. The as-coated film was baked at 150  $^\circ\text{C}$  for 3 min and then annealed in air atmosphere for 15 min in a box furnace. The annealing temperature was changed from 300  $^\circ\text{C}$  to 900  $^\circ\text{C}$  to obtain a single-layer  $\text{SiO}_x$  sample (as shown in Fig. 1 (a)); as for the structure of the stack layer, after depositing  $\text{SiO}_x$  film on the front and back surfaces of the silicon wafer and annealing, PE-ALD  $\text{AlO}_x$  with a thickness of 15 nm (as shown in Fig. 1(B1)) and an 80 nm PECVD  $\text{SiN}_x$  layer (Fig. 1(B2)) were capped on the  $\text{SiO}_x$  layers. Single  $\text{AlO}_x$  and  $\text{SiN}_x$  layers passivated silicon wafer were used as references. The  $\text{SiO}_x/\text{AlO}_x:\text{H}$  stack shown in Fig. 1(C) was obtained by exchanging the preparing order of  $\text{AlO}_x$  and  $\text{SiO}_x$ . After two-side deposition on silicon wafer, the single  $\text{AlO}_x$ ,  $\text{SiO}_x/\text{AlO}_x:\text{H}$ , and  $\text{SiO}_x/\text{AlO}_x:\text{H}$  stacks were annealed at 400  $^\circ\text{C}$  for 10 min, and  $\text{SiN}_x$  layers,  $\text{SiN}_x/\text{SiO}_x:\text{H}$ , were annealed at 450  $^\circ\text{C}$  for 10 min in atmosphere.  $\text{AlO}_x$  layers were deposited at 200  $^\circ\text{C}$  with TMA and oxygen as the reaction precursor, and PECVD  $\text{SiN}_x$  layers were deposited at 400  $^\circ\text{C}$  with  $\text{SiH}_4$  and  $\text{NH}_3$  as the reaction precursor. The components and the thickness of the film were tested by Fourier transform infrared spectroscopy (FTIR) spectroscopy and ellipsometer, respectively. The effective minority carrier lifetime of a passivated silicon wafer and fixed charge in the dielectric film were measured through transient micro-photoconductive decay using WT-2000 instrument. The distribution of H in the film was tested by Time of Flight Secondary Ion Mass Spectrometry

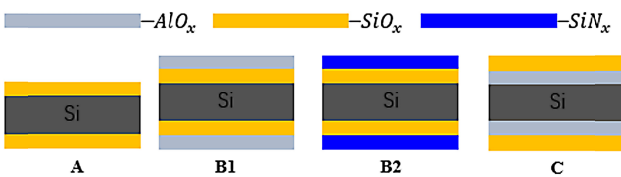


Fig. 1. Sample structures in the experiment; A is the structure of single  $\text{SiO}_x$ -passivated Si wafer, B1 is a double-sided  $\text{SiO}_x/\text{AlO}_x:\text{H}$  stack-passivated Si wafer, B2 is a  $\text{AlO}_x/\text{SiO}_x:\text{H}$  stack-passivated Si wafer, and C is a  $\text{SiO}_x/\text{SiN}_x:\text{H}$ -passivated Si wafer. (TOF-SIMS).

## III. RESULTS AND DISCUSSIONS

### A. Film components

The absorption FTIR spectra of the  $\text{SiO}_x$  film before and after annealing are shown in Fig. 2. This shows that the chemical component changes after annealing. The spectra for the as-deposited sample show the absorption peaks associated with the N-H peak (3,400  $\text{cm}^{-1}$ ), the Si-H peak (2,145  $\text{cm}^{-1}$ ), Si-O peak (1,080  $\text{cm}^{-1}$ ), and the Si-N peak (860  $\text{cm}^{-1}$ ). After

annealing at 300  $^\circ\text{C}$  for 15 min, the N-H and Si-H peaks almost disappeared, whereas the Si-O peak intensity increased significantly, and the Si-N peak still appeared with lower intensity. As the annealing temperature increased, the intensity of the Si-O peak became higher, and the Si-N peak remained at a low level. This reveals that the Si-N, N-H, and Si-H bonds were broken, and the Si-O bond was formed by Si bonds reacting with the oxygen in the atmosphere during annealing.

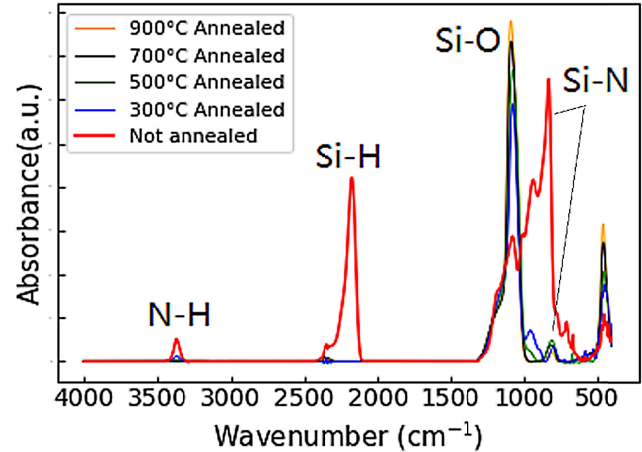


Fig. 2. The FTIR spectrum for  $\text{SiO}_x$  (280 nm) before and after annealing

Fig. 3 shows the peak of the Si-O normalized by Si-N peak (a) and the ratio of the Si-O peak's height to the Si-N peak's height (b) as a function of the annealing temperature. Their peak position moves toward a higher wavenumber with increasing annealing temperature; this indicates that the composition of the film is closer to chemical stoichiometry  $\text{SiO}_2$ . When the annealing temperature is up to 600  $^\circ\text{C}$ , the ratio of Si-O bond increases significantly, indicating that the Si-N bond more easily transfers to the Si-O bond under higher temperature. The PHPS film could be defined as  $\text{SiO}_x\text{N}_y:\text{H}$ , the atomic ratios of Si, O, and N can be calculated from the area of the Si-O and Si-N peaks in the FTIR spectrum. For the composition of  $\text{SiO}_x\text{N}_y$ , x and y satisfy the following relationship [15]:

$$x = \frac{[\text{O}]}{[\text{Si}]} = \frac{2[\text{Si} - \text{O}]}{[\text{Si} - \text{O}] + [\text{Si} - \text{N}]}$$

and

$$y = \frac{[\text{N}]}{[\text{Si}]} = \frac{4}{3} \cdot \frac{2[\text{Si} - \text{N}]}{[\text{Si} - \text{O}] + [\text{Si} - \text{N}]}$$

$[\text{Si} - \text{X}]$  is the absolute concentration of the bond and can be calculated by  $[\text{Si} - \text{X}] = K_{\text{Si-X}} \int_v \frac{\alpha(\omega)}{\omega} d\omega = K_{\text{Si-X}} A_{\text{Si-X}}$ , the coefficient  $K_{\text{Si-O}} = 1.5 \times 10^{19} \text{ cm}^{-2}$ , and  $K_{\text{Si-N}} = 2.1 \times 10^{19} \text{ cm}^{-2}$ . After calculating the value of  $[\text{O}] / [\text{Si}]$  and  $[\text{N}] / [\text{Si}]$ , we find that x continues to increase and y continues to decrease as the annealing temperature increases. The value of x is 1.95 at 300 $^\circ\text{C}$  and 1.98 at 900 $^\circ\text{C}$ , and that of y changes from 0.07 to 0.02. Therefore, the result reveals that N and H are released to the outside of the film in the form of  $\text{H}_2$  and  $\text{NH}_3$  during annealing, and the components of the film are mainly dominated by Si-O bonds. So, the film is gradually changed to the stoichiometric  $\text{SiO}_2$  during annealing.

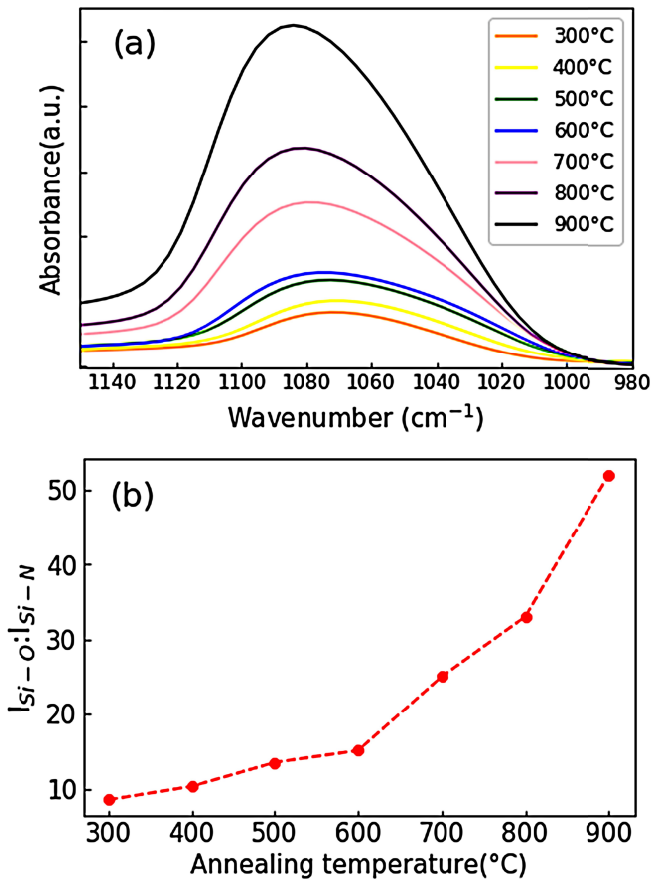


Fig. 3. FTIR spectrum of films annealed at different temperatures are normalized with the height of the Si-N peak and are shown in (a); the height ratio of Si-O and Si-N peaks varying with annealing temperature is shown in (b); the dash line is only for guidance.

### B. Surface passivation quality

The effective minority carrier lifetime  $\tau_{\text{eff}}$  for 280 nm SiO<sub>x</sub> as a function of annealing temperature is shown in Fig. 4. In the low temperature range (200–500 °C), the value of  $\tau_{\text{eff}}$  is quite small and rise slightly; then,  $\tau_{\text{eff}}$  increases significantly to more than 1200  $\mu\text{s}$  at 700 °C. However,  $\tau_{\text{eff}}$  begins to decrease as the temperature further increases to 800 °C and above. To find the reasons for the decline, the corona charge test was performed on the films.

The corona charge method is a non-contact measurement method. By applying a charge of opposite polarity to the fixed charge  $Q_f$  to the surface of the sample, the field effect passivation is weakened, and the minority carrier lifetime is thus lowered; as the charge is continuously applied, the excess charge provides a passivation effect that causes  $\tau_{\text{eff}}$  to begin to rise, forming a complete corona charge curve as shown in Fig. 5. The amount of charge applied at the lowest point of the curve is approximately regarded as the interface fixed charge  $Q_f$ , and the minimum effective minority carrier lifetime ( $\tau_{\text{min}}$ ) of the curve corresponds to the effect of chemical passivation, which is related to the interface state density  $D_{it}$ .

Fig. 7 shows that the fixed charge density is approximately  $+1\sim 2 \times 10^{12} \text{ cm}^{-2}$ , which is much higher than that in thermal

oxidation of SiO<sub>2</sub> of  $+3 \times 10^{11} \text{ cm}^{-2}$ [16]. The charge density gradually increases as the temperature increases, so the film annealed at higher temperature has better field effect passivation. As for the  $\tau_{\text{min}}$ , it is approximately 1/10 of  $\tau_{\text{eff}}$  for all the temperatures; so, the chemical passivation is very limited. The figure also shows that the relationship between  $\tau_{\text{min}}$  and temperature is quite similar to that of  $\tau_{\text{eff}}$  and temperature.

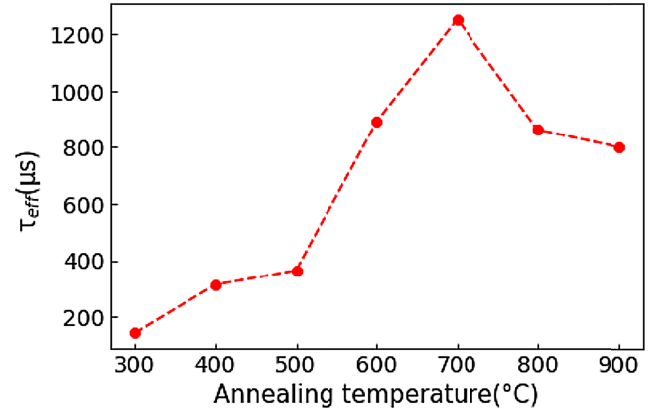


Fig. 4. The effective minority carrier lifetime of a 280 nm SiO<sub>x</sub> varies with annealing temperature; the dash line is only for guidance.

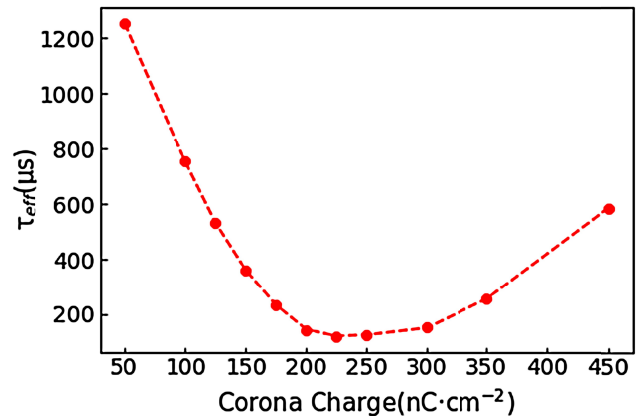


Fig. 5. An example of the corona charge curve of 280 nm SiO<sub>x</sub> film annealed at 700°C.

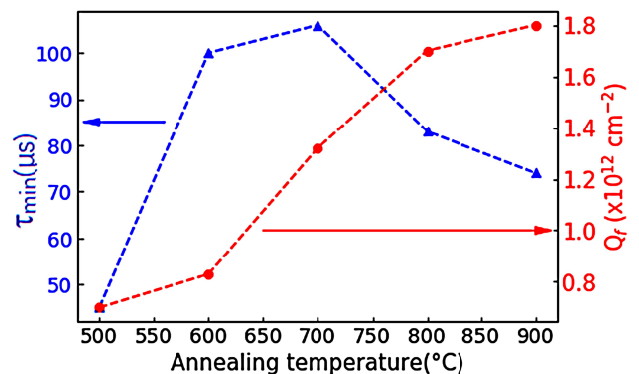


Fig. 6. •  $\tau_{\text{min}}$  and  $Q_f$  for the 280 nm single-layer SiO<sub>x</sub>-passivated silicon wafer annealed at different temperatures; the dashed line is only for guidance.

Therefore, it can be concluded that the decrease of  $\tau_{\text{eff}}$  at 800–900 °C mainly because of the increase of  $D_{it}$ . So we chose

the temperature of 700 °C as the annealing temperature for single SiO<sub>x</sub> layer in the following study.

The relationship between film thickness and dilution ratio of PHPS with N-butyl ether is shown in Fig. 7. As the dilution ratio increases, the thickness of the film gradually decreases from 280 nm to less than 10 nm. The  $\tau_{\text{eff}}$  as a function of the film thickness is plotted in Fig. 8. When the film is thinner than 15 nm,  $\tau_{\text{eff}}$  is maintained at approximately 220  $\mu\text{s}$ ; then,  $\tau_{\text{eff}}$  increases quickly as the film thickness increases and reaches 1100  $\mu\text{s}$  at 80 nm. As the film thickness continuously increases, the upward trend of  $\tau_{\text{eff}}$  becomes slow and reaches 1250  $\mu\text{s}$  at 280 nm. It has been pointed out that when the lower thickness of the PHPS is thermal-treated, the film formation is less uniform, and cracks are likely to occur; this may be a cause of the serious decrease in the passivation effect[17].

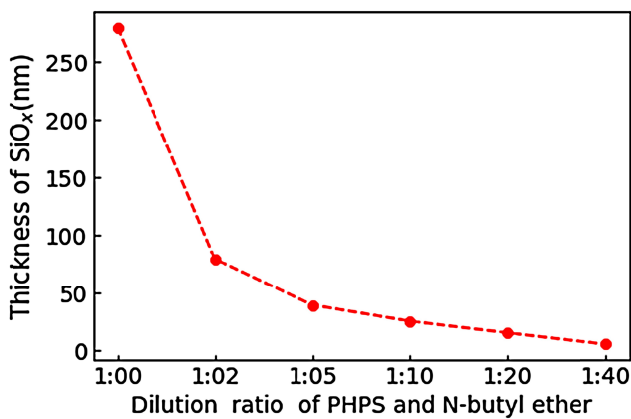


Fig. 7. The thickness of SiO<sub>x</sub> varies with dilution ratio after annealing at 700 °C for 15 min.

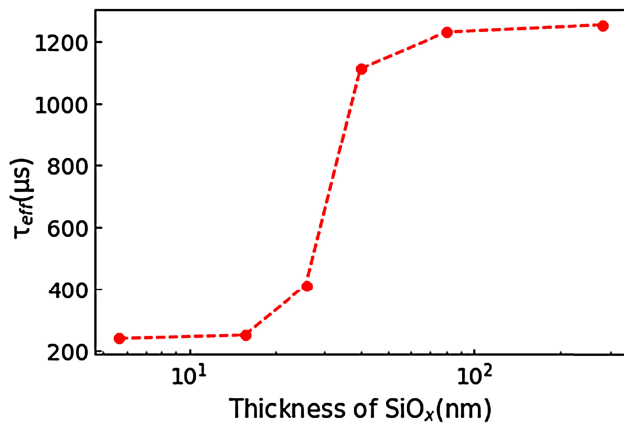


Fig. 8. Effective minority carrier lifetime as a function of single SiO<sub>x</sub> layer's thickness after annealing at 700 °C for 15 min.

To investigate the passivation properties of the SiO<sub>x</sub> film combining with other passivation layers, we prepared the stack layers of SiO<sub>x</sub>/AlO<sub>x</sub>:H and SiO<sub>x</sub>/SiN<sub>x</sub>:H, in which SiO<sub>x</sub> is close to the silicon surface and AlO<sub>x</sub>, SiN<sub>x</sub> is the cap layer. It should be noted that for the stack layer, after studying the effect of annealing temperature of SiO<sub>x</sub> layer on the surface passivation quality of SiO<sub>x</sub>/AlO<sub>x</sub>:H and SiO<sub>x</sub>/SiN<sub>x</sub>:H, we found the optimized annealing temperature of SiO<sub>x</sub> to be 450 °C. Then, in the stacks preparation, the annealing of SiO<sub>x</sub> was conducted at 450 °C. The SiO<sub>x</sub>/AlO<sub>x</sub>:H stack was prepared with different

thicknesses of the SiO<sub>x</sub> film, whereas for SiO<sub>x</sub>/SiN<sub>x</sub>:H, the thicknesses of SiO<sub>x</sub> and SiN<sub>x</sub> were fixed at 280 nm and 80 nm, respectively. The result for SiO<sub>x</sub>/AlO<sub>x</sub>:H is shown in the Fig. 9. The function of effective minority carrier lifetime with SiO<sub>x</sub> thickness is basically the same as that of single SiO<sub>x</sub> layer. It is evident that  $\tau_{\text{eff}}$  values for SiO<sub>x</sub>/AlO<sub>x</sub>:H stack-passivated silicon wafers are higher than those for SiO<sub>x</sub>; however, in the case of smaller thickness, the passivation effect is very limited, whether it is a SiO<sub>x</sub> film (as shown in Fig. 8) or an SiO<sub>x</sub>/AlO<sub>x</sub>:H stack; for example, the SiO<sub>x</sub> layer's thickness is smaller than 50 nm, and the stack layers have a poorer surface passivation effect compared with single AlO<sub>x</sub> layer ( $\tau_{\text{eff}} \approx 750 \mu\text{s}$ ). However, the  $\tau_{\text{eff}}$  of the stack layer exceeds that of AlO<sub>x</sub> as the SiO<sub>x</sub> thickness is more than 50 nm; furthermore, it can reach more than 2200  $\mu\text{s}$  when the thickness of SiO<sub>x</sub> is 80 nm or more, whereas the value is approximately 1 ms for single 80 nm SiO<sub>x</sub>. The interface fixed charge of the stack measured by a corona charge method is maintained at approximately  $+3 \times 10^{11} \text{ cm}^{-2}$  when the SiO<sub>x</sub> thickness is above 80 nm. Compared with single SiO<sub>x</sub> layer,  $Q_f$  of the SiO<sub>x</sub>/AlO<sub>x</sub>:H stack is significantly lower, but the  $\tau_{\text{min}}$  of the stack is 10 times higher than that of the SiO<sub>x</sub> film; this means that the chemical passivation is much stronger. As a result, the field effect passivation is relatively weakened, but with higher chemical passivation in the stack. By comparing the FTIR spectrum of the SiO<sub>x</sub> film and SiO<sub>x</sub>/AlO<sub>x</sub>:H stack, we find that the FTIR of the SiO<sub>x</sub> film after annealing at 450 °C does not show obvious peaks at 2200  $\text{cm}^{-1}$  (Si-H), but the SiO<sub>x</sub>/AlO<sub>x</sub>:H stack does (not shown here). This may indicate that the diffusion of hydrogen from AlO<sub>x</sub> films during annealing saturates the dangling bonds on the surface of the substrate to eliminate such recombination centers. To investigate the distribution of H in the stack, we used a TOF-SIMS test and got the spectrum of the SiO<sub>x</sub> (80 nm)/AlO<sub>x</sub> (15 nm) stack as shown in Fig. 10; a result of a 15 nm AlO<sub>x</sub> film is used as reference. In the single AlO<sub>x</sub> film, the intensity of H<sup>+</sup> and SiH<sup>+</sup> remains at a low value and begins to increase until at the surface of Si. As for the stack of SiO<sub>x</sub>/AlO<sub>x</sub>:H, there are more H<sup>+</sup> or SiH<sup>+</sup> bonds in the SiO<sub>x</sub> layer than in AlO<sub>x</sub> layer, and an evident peak exists at the position closer to the substrate, even though the Si-H bonds in SiO<sub>x</sub> have disappeared after annealing at 450 °C, which means that the H in AlO<sub>x</sub> can diffuse into the SiO<sub>x</sub> layer and accumulate at the surface of the Si substrate. This H saturates the dangling bonds to reduce  $D_{it}$  and achieve effective chemical passivation. In other words, this confirms that the excellent passivation of the SiO<sub>x</sub>/AlO<sub>x</sub>:H stack was mainly due to the enhancement of chemical passivation. This implies that higher concentration of H effusing from the AlO<sub>x</sub> layer can be stored in the SiO<sub>x</sub> layer, especially at the SiO<sub>x</sub>/Si interface; these higher H concentrations provide better chemical passivation on silicon's surface than that passivated by single SiO<sub>x</sub> and AlO<sub>x</sub> layers. However, combining the TOF-SIMS results with the  $\tau_{\text{eff}}$  result of the SiO<sub>x</sub>/AlO<sub>x</sub>:H stack shown in Fig. 9, it could be concluded that the effective effusion and storage H in SiO<sub>x</sub> should require that the thickness of SiO<sub>x</sub> is not less than 50 nm, and the thickness has less influence when the it closes 100 nm or more. It is interesting that when coating 80 nm SiO<sub>x</sub> on 15 nm AlO<sub>x</sub> and after annealing at 400 °C for 10 min, the minority carrier lifetime also increased from 750  $\mu\text{s}$  for the AlO<sub>x</sub> layer to about

1,200  $\mu\text{s}$  for the stack. The  $Q_f$  values in  $\text{AlO}_x/\text{SiO}_x\text{:H}$  and  $\text{AlO}_x$  are identical; this means that reduced  $D_{it}$ , which results from the hydrogenation of the Si surface, contributes to the improvement of surface passivation on silicon.

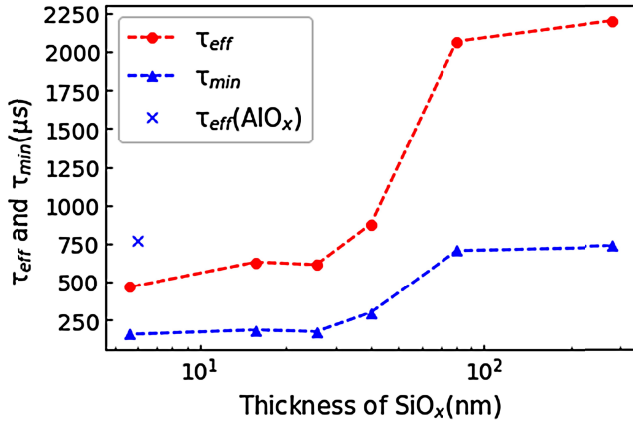


Fig. 9.  $\tau_{\text{eff}}$  and  $\tau_{\text{min}}$  of the  $\text{SiO}_x/\text{AlO}_x\text{:H}$  stack varies with thickness of  $\text{SiO}_x$ . Before the deposition of 15 nm  $\text{AlO}_x$ ,  $\text{SiO}_x$  were annealed at  $450^\circ\text{C}$  for 15 min. The stacks received extra annealing at  $400^\circ\text{C}$  for 10 min. The  $\tau_{\text{eff}}$  of 15 nm single-layer  $\text{AlO}_x$  annealed at  $400^\circ\text{C}$  for 10 min is the reference.

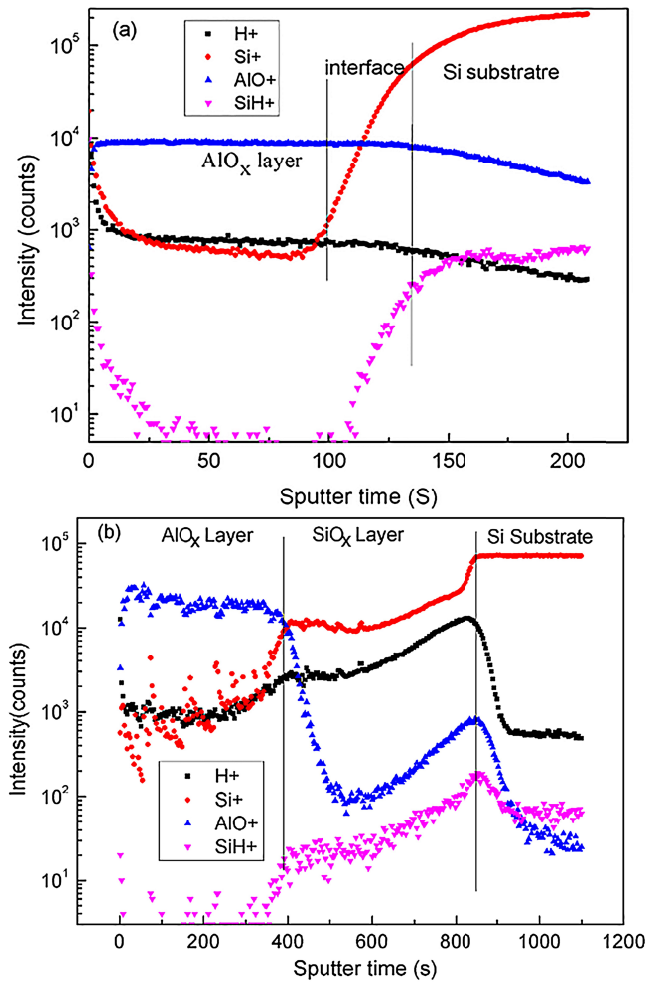


Fig. 10. TOF-SIMS spectra of single  $\text{AlO}_x$  layer (a) and the  $\text{SiO}_x/\text{AlO}_x\text{:H}$  stack (b), in which  $\text{AlO}_x$  is a 15 nm thick layer annealed at  $400^\circ\text{C}$  for 10 min. Before deposition of  $\text{AlO}_x$ , 80 nm  $\text{SiO}_x$  was annealed at  $450^\circ\text{C}$ . The stacks received extra annealing at  $400^\circ\text{C}$  for 10 min. The boundaries of the passivation layer, the Si substrate and the interface are indicated by the vertical line.

As for the  $\text{SiO}_x/\text{SiN}_x\text{:H}$  stack, 280nm  $\text{SiO}_x$  was coated and annealed at  $450^\circ\text{C}$  for 15min; then, 80nm  $\text{SiN}_x$  was then deposited by PECVD and then annealed at  $450^\circ\text{C}$  for 10min. The result shows that the insertion of  $\text{SiO}_x$  between the substrate and  $\text{SiN}_x$  can increase the minority carrier lifetime from 422  $\mu\text{s}$  ( $\text{SiN}_x$ ) to 1,627  $\mu\text{s}$ . The fixed charge density of the stack is approximately  $+2 \times 10^{12} \text{ cm}^{-2}$ , which is nearly the same as that of  $\text{SiO}_x$  and less than that of  $\text{SiN}_x$  ( $+3 \times 10^{12} \text{ cm}^{-2}$ ). The  $\tau_{\text{min}}$  of  $\text{SiO}_x/\text{SiN}_x\text{:H}$  stack is approximately 500  $\mu\text{s}$ . The result of the corona charge measurement indicates that the field effect passivation of the  $\text{SiO}_x/\text{SiN}_x\text{:H}$  stack is substantially the same as that of the  $\text{SiO}_x$  film, and the chemical passivation effect is fairly substantial. This also confirms that  $\text{SiO}_x$  is the barrier of H effusion to the outside of stack layers. Therefore, the single  $\text{SiO}_x$  film has strong field-effect passivation provided by the  $Q_f$ , and its chemical passivation effect is limited. However, the  $\text{SiO}_x/\text{AlO}_x\text{:H}$  or  $\text{SiO}_x/\text{SiN}_x\text{:H}$  stack can effectively compensate for its disadvantage of chemical passivation.

## IV. CONCLUSIONS

In conclusion, we have studied a new method for preparing silicon oxide by spin-coating PHPS film with some heat treatments. During PHPS films are annealed, the Si–O bonds are formed, and N and H are released to the outside to form a SiO<sub>x</sub> film. The new SiO<sub>x</sub> shows excellent passivation properties: the effective minority carrier lifetime increases with SiO<sub>x</sub> thickness and can reach 1 ms when thickness is up to 100 nm. Moreover, when 100 nm or thicker SiO<sub>x</sub> layers were capped by a AlO<sub>x</sub> or SiN<sub>x</sub> layer, the effective minority carrier lifetime could get the value above 2 ms, which is much higher than the value for single SiN<sub>x</sub> or AlO<sub>x</sub> (approximately 500–750 μs). The large density of positive fixed charge provides good field effect passivation and the diffusion of H from the AlO<sub>x</sub> or SiN<sub>x</sub> layer toward the silicon surface provides chemical passivation. The new SiO<sub>x</sub> has quite a simple preparation process and requires low temperature compared with traditional ways. These advantages on preparation and performance provide good development potential and application prospects.

## REFERENCES

- [1] E. Cartier, J. H. Stathis, and D. A. Buchanan, "Passivation and depassivation of silicon dangling bonds at the Si/SiO<sub>2</sub> interface by atomic hydrogen," *Appl. Phys. Lett.*, vol. 63, no. 11, pp. 1510-1512, 1993.
- [2] J. G. Fossum, R. P. Mertens, D. S. Lee, and J. F. Nijs, "Carrier recombination and lifetime in highly doped silicon," *Solid-State Electron.*, vol. 26, no. 6, pp. 569-576, 1983.
- [3] P. Ericsson, S. Bengtsson, and J. Skarp, "Properties of Al<sub>2</sub>O<sub>3</sub> films deposited on silicon by atomic layer epitaxy," *Microelectron. Eng.*, vol. 36, no. 1, pp. 91-94, 1997.
- [4] Y.R. Xiang, C.L. Zhou, E.D. Jia, and W.J. Wang, "Oxidation precursor dependence of atomic layer deposited Al<sub>2</sub>O<sub>3</sub> films in a-Si:H(i)/Al<sub>2</sub>O<sub>3</sub> surface passivation stacks," *Nanoscale Res. Lett.*, vol. 10, no. 1, pp. 137, 2015.
- [5] J.A. Töfflinger, A. Laades, C. Leendertz, L.M. Montañez, L. Korte, B. Rech, U. Stürzebecher, H.P. Sperlich, "PECVD-AlO<sub>x</sub>/SiN<sub>x</sub> Passivation Stacks on Silicon: Effective Charge Dynamics and Interface Defect State Spectroscopy," *Energy Procedia*, vol. 55, pp. 845-854, 2014.
- [6] M. L. Reed, and J. D. Plummer, "Chemistry of Si• SiO<sub>2</sub> interface trap annealing," *J. Appl. Phys.*, vol. 63, no. 12, pp. 5776-5793, 1988.
- [7] S. W. Glunz, D. Biro, S. Rein, and W. Warta, "Field-effect passivation of the SiO<sub>2</sub>-Si interface," *J. Appl. Phys.*, vol. 86, no. 1, pp. 683-691, 1999.
- [8] H. Angermann, "Conditioning of Si-interfaces by wet-chemical oxidation: Electronic interface properties study by surface photovoltage measurements," *Appl. Surf. Sci.*, vol. 312, pp. 3-16, Sep 1, 2014.
- [9] B. E. Deal, and A. S. Grove, "General relationship for thermal oxidation of silicon," *J. Appl. Phys.*, vol. 36, no. 12, pp. 3770-&, 1965, 1965.
- [10] D. W. Hess, "Plasma assisted oxidation, anodization, and nitridation of silicon," *IBM J. Res. Dev.*, vol. 43, no. 1-2, pp. 127-145, Jan-Mar, 1999.
- [11] A. Moldovan, F. Feldmann, M. Zimmer, J. Rentsch, J. Benick, and M. Hermle, "Tunnel oxide passivated carrier-selective contacts based on ultra-thin SiO<sub>2</sub> layers," *Sol. Energy Mater. Sol. Cells*, vol. 142, pp. 123-127, 2015.
- [12] O. Funayama, Y. Tashiro, A. Kamo, M. Okumura, and T. Isoda, "Conversion mechanism of perhydropolysilazane into silicon nitride-based ceramics," *J. Mater. Sci.*, vol. 29, no. 18, pp. 4883-4888, 1994.
- [13] J.A. Töfflinger, A. Laades, C. Leendertz, L.M. Montañez, L. Korte, B. Rech, U. Stürzebecher, H.P. Sperlich, "Conversion of perhydropolysilazane into a SiO<sub>x</sub> network triggered by vacuum ultraviolet irradiation: access to flexible, transparent barrier coatings," *Chemistry*, vol. 13, no. 30, pp. 8522-8529, 2010.
- [14] H. Nagayoshi, and T. Murooka, "TiO<sub>2</sub> Nanoparticle/SiO<sub>2</sub> Composite Back Reflector for Solar Cells," *Energy Procedia*, vol. 77, pp. 242-247, 2015.
- [15] J. C. Rostaing, Y. Cros, S. C. Gujrathi, and S. Poulain, "Quantitative infrared characterization of plasma enhanced CVD silicon oxynitride films," *J. Non-Cryst. Solids*, vol. 97, no. 87, pp. 1051-1054, 1987.
- [16] H. Haug, S. Olibet, O. Nordseth, and E. Stensrud Marstein, "Modulating the field-effect passivation at the SiO<sub>2</sub>/c-Si interface: Analysis and verification of the photoluminescence imaging under applied bias method," *J. Appl. Phys.*, vol. 114, no. 17, pp. 174502, 2013.
- [17] W. Kwon, "Preparation of Silicon Carbide Oxidation Protection Film on Carbon Thermal Insulator Using Polycarbosilane and Its Characterization," *Korean J. Mater. Res.*, vol. 27, no. 9, pp. 471-476, 2017, 2017.



**L. Gong** was born in Hunan, China in 1994. He received Bachelor degree from Tsinghua University in 2016. He is currently pursuing the Master's degree in Institute of Electrical Engineering, Chinese Academy of Science, Beijing, China.



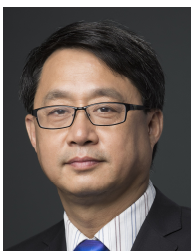
**C.L. Zhou** was born in China in 1977. She received the bachelor degree from Lanzhou University in 2000 and the doctoral degree from the institute of High Energy Physics, Chinese Academy of Science in 2005.

From 2005 to 2006, she was a Lecturer with the Institute of Low Energy Nuclear Physics, Beijing Normal University. Since 2006, she has been a Professor with Institute of Electrical Engineering, Chinese Academy of Sciences (IEECAS), focusing on production technology of the high efficiency laser grooved buried contact single-crystal solar cell, high efficiency crystal solar cell, the potential induced degradation of solar cell, black silicon solar cell and new generation solar cells.



**J.J. Zhu** received the Ph.D. degree in optoelectronic material preparation and characterization from the University of Science and Technology of China, Hefei, China, in 2005.

Since 2009, he has been a Research Scientist with the Institute for Energy Technology, Kjeller, Norway, focusing on the development of high-efficiency Si solar cells with different concepts, for instance, passivated emitter and rear cells, metal-wrap through, and interdigitated back contact.



**W.J. Wang** received Ph.D. degree from Changchun Institute of Physics, Chinese Academy of Sciences in 1994. From 1994 to 1996, he conducted postdoctoral research at the Institute of Chemistry of the Chinese Academy of Sciences.

After entering the Beijing Solar Energy Research Institute in 2006, he has been engaged in research on solar cells. Since 2005, he has been working in the Institute of Electrical Engineering, Chinese Academy of Sciences as the group leader of the Key Laboratory of Solar Thermal Energy and Photovoltaic System, Institute of Electrical Engineering, Chinese Academy, Beijing, China. His main research directions are: high efficient silicon solar cells, solar cell industry policy, solar cell electricity price policy, solar cell application development.

Dr. Wang is a member of China Solar Energy Society, China Solar Energy Society Photovoltaic Professional Committee and the Photovoltaic Professional Committee of China Standardization Society.